

Effect of plastic fines on the small strain stiffness of sand

El Mohtar, C.S., Santagata, M., Bobet, A., Drnevich, V.P.

School of Civil Engineering, Purdue University, W. Lafayette, IN

Johnston, C.

Department of Agronomy, Purdue University, W. Lafayette, IN

Keywords: shear modulus, aging, plastic fines, small strains, sand

ABSTRACT: The paper investigates the small strain shear stiffness (G_{max}) of sand-bentonite specimens (0, 3 and 5% bentonite by dry mass of the sand) prepared at the same skeleton void ratio (corresponding to $D_{rsk}=35-40\%$) using a dry pluviation technique. Based on resonant column tests performed at very small strains at increasing stress levels (25-300 kPa), it is found that the same type of relationship links the initial stiffness (G_{max}) to stress level and skeleton void ratio, with the presence of fines leading to only a marginal decrease in G_{max} . This effect can be ascribed to the presence of bentonite at the sand grain contacts. The paper also presents G_{max} data obtained over time (up to approximately 7 days), which show that the presence of 3% and 5% bentonite increases the aging coefficient (N_G) by a factor of 2 and 3, respectively. Finally the paper examines the values of the shear wave velocity (V_s) measured on the sand-bentonite specimens and draws attention to the potential problems in employing this soil property as an index of liquefaction resistance in soils with small percentages of highly plastic fines.

1 INTRODUCTION

Contradictory results are presented in the literature on the effects of fines on both the shear strength and the cyclic resistance of sands (Carraro et al. 2003; Polito and Martin 2003; Thevanayagam et al. 2002). This can be in part attributed to the different types of microstructure that are formed in these soils depending on the amount and the nature of the fines, as well as to the use of different void ratio parameters (bulk versus skeleton void ratio) in the analysis of the data. Different researchers argue for the use of one parameter over the other for the characterization of sands with fines.

Finn et al. (1994), Vaid (1994) and Thevanayagam et al. (2002) all report that, provided that the percentage of fines is smaller than a critical value, the shear strength is relatively independent of the fines content when the skeleton void ratio is used as the specimen density controlling parameter. Similar observations have been reported by Georgiannou et al. (1991) for clayey sands. The critical value of the fines content depends on the nature of the fines as well as on the characteristics and relative density of the sand. Below the critical value the fines fill the voids between the sand particles and the small strain behavior is controlled by the sand grain to grain contacts (Thevanayagam

et al. 2002). At higher fine contents a “floating” fabric is generated instead (Thevanayagam and Martin, 2002) and the sand particles do not touch each other resulting in a weaker structure.

In this study, resonant column tests were performed on sand specimens prepared at relatively high skeleton void ratios (0.66 to 0.70) with no fines as well as with 3% and 5% bentonite (by mass of the sand). G_{max} data were obtained over a range of consolidation stresses (25-300 kPa) for aging times up to 7 days. Additional measurements were conducted on selected specimens over the various stages of the resonant column tests from setup, to flushing and hydration, to consolidation and creep.

The results of the resonant column tests are used to examine the influence of small percentages of highly plastic fines on G_{max} , and on the dependence of this parameter on stress level, void ratio and time. Additionally the data are used to gain insight into the fabric that is formed in dry mixed sand-bentonite specimens, and to illustrate how the specimen preparation method plays an important role in determining the microstructure and, hence, the stiffness of the soil.

Finally, the paper employs the shear wave velocity data to discuss the use of this parameter as a measure of the liquefaction susceptibility of soils.

2 EXPERIMENTAL PROGRAM

2.1 Material

All tests performed for this study made use of graded Ottawa sand C 778: a uniform ($C_u=1.7$) and clean fine to medium sand ($D_{50} = 0.4\text{mm}$), with 2-5% finer than 0.075 mm, specific gravity $G_s = 2.65$, and maximum and minimum void ratios $e_{\max} = 0.78$ and $e_{\min} = 0.48$. The bentonite used is a Wyoming bentonite (CP-200), commercialized by VOLCLAY, with at least 70% finer than 0.075 mm, and minimum free swell of 8 ml/g. Deionized deaired water was used to flush and saturate the resonant column specimens.

2.2 Resonant column tests

All resonant column tests in this study were performed using the Drnevich resonant column apparatus (Drnevich et al. 1978) available in the Bechtel Geotechnical Laboratory at Purdue University. Tests were performed to determine both the initial shear modulus (G_{\max}) at very small strains ($\sim 10^{-4}\%$), and the stiffness degradation behavior (not presented in this paper).

The test apparatus was modified to enable top and bottom drainage, so that the specimens prepared through the dry mixing technique (see below) could be flushed first with carbon dioxide and then with water, and subsequently backpressure saturated.

Additionally, the vertical alignment ball-bearing component in the resonant column was removed to reduce friction and allow for more accurate measurements at very low strains. To compensate for the absence of the vertical ball-bearings, additional care was taken in specimen preparation. Figure 1 shows the modified top platen of the resonant column. The figure shows the added top drainage line and no vertical alignment. As a result of this modification, outside of the fixed base, the only physical contact between the specimen and the loading system is through a tension spring with very low torsional resistance at the top of the specimen. Such a configuration allows for a true fixed base-free rotating top modeling of the system.

The specimen preparation method was modified from standard procedures (ASTM D 4015) to accommodate the specific nature of the tested materials. In this method the sand and the desired percentage of bentonite are dry mixed in an airtight container for 15 minutes and air-pluviated using a funnel in a triaxial split mold ($D=70$ mm, $H=200$ mm), to prepare 160 mm tall specimens. The mold is then tapped on the sides to achieve the desired skeleton void ratio ($e_{\text{sk}} = [V_{\text{tot}} - V_{\text{sand}}]/V_{\text{sand}}$). For all the tests presented in this paper the same skeleton relative density ($35\% \pm 5\%$) was targeted ($D_{r_{\text{sk}}} = [e_{\max} - e_{\text{sk}}]/[e_{\max} - e_{\min}]$, with e_{\max} and e_{\min}

determined on the clean sand). The specimen is then set under a 25 kPa effective confining stress by applying vacuum until the cell is assembled and an equivalent cell pressure can be applied. Then, it is flushed from bottom to top first with carbon dioxide (CO_2), and then with deionized deaired water.

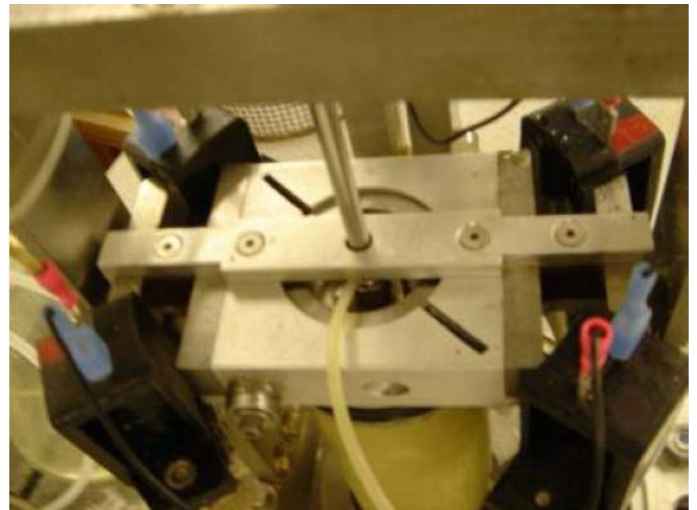


Figure 1: Modified setup of the resonant column with top drainage and no vertical alignment

The specimen preparation and flushing were conducted with special attention to avoid early hydration of the bentonite that would interfere with uniform saturation of the mixture. Specifically, the sand-bentonite mixture was air pluviated into the mold with all drainage lines/porous stone/filter papers dry to prevent the bentonite from getting in contact with water before the flushing phase. Additionally, flushing was completed over a short period of time (< 2 h) under increasing gradients (maximum hydraulic gradient of 5) to maintain constant water flow through the specimen. These procedures allowed uniform flushing of water and prevented caking at the base of the specimens. Hydrometer tests conducted on soil obtained from different locations inside selected soil specimens showed the bentonite content to be within $\pm 0.25\%$ (by mass of dry sand) of the target value. The void ratio distribution was estimated from the variation in water content at the top, center and bottom of the specimen. The results showed that the values of the void ratios at the different locations were within $\pm 2.5\%$ of the specimen average void ratio.

Following flushing the clean sand specimens are back pressure saturated for 24 hours with a back pressure of 200-400 kPa to achieve B-values > 0.95 (following recommendations by Black and Lee, 1973), while the sand-bentonite specimens are allowed a 72 hours rest period to ensure full hydration and swelling of the bentonite inside the sand pores. The selection of the duration of the rest phase is based on a study of the swelling time and swelling pressure of sand-bentonite mixtures, which shows that a minimum time of 36 hours is needed

for the bentonite in the pores to hydrate and swell under atmospheric pressure (El Mohtar, 2008). After the rest period the sand-bentonite specimens are back-pressure saturated, using the same procedure as the clean sand; following saturation, all specimens are isotropically consolidated to the desired effective consolidation stress (50–300 kPa for the tests presented in this paper).

3 RESULTS

3.1 Effects of flushing and hydration on G_{max} of sand-bentonite specimens

The small-strain shear stiffness (at strain amplitudes of $10^{-4}\%$) of select specimens was monitored during the different stages of a resonant column test: flushing and hydration, back pressure saturation and consolidation. Figures 2 and 3 present the results obtained for two specimens: one of clean sand and one with 3% bentonite. The plots are representative of results obtained in other tests. The three plots

shown in each of these figures portray the values of G_{max} as a function of time from the beginning of each of the three main stages of the test outlined above. Note that for comparison purposes, the sand specimen used for the test shown in Figure 2 was allowed a 72 hour rest period prior to saturation as in the case of the specimens with bentonite (for typical tests performed on clean sand, the saturation stage started immediately after flushing with water). These results offer interesting insight on the fabric of the specimens and on the mechanisms responsible for the measured stiffness. The arrows in Figures 2 and 3 indicate the end of the dry, flushing and hydration stages.

Figure 2 shows no significant change in the stiffness of the clean sand specimen during flushing with water (the time shown on the x-axis is taken from the time of application of the 25 kPa cell pressure). This is expected because at very low strains, the stiffness is controlled by the particle to particle contacts. Given that water is flushed through the specimen at a low gradient, particle contacts are

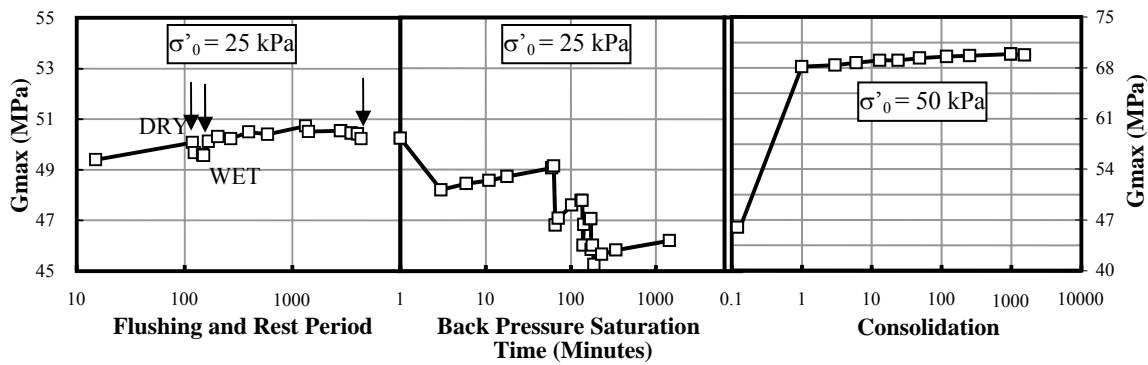


Figure 2: Monitoring of G_{max} throughout the different stages of a resonant column test on a clean sand specimen

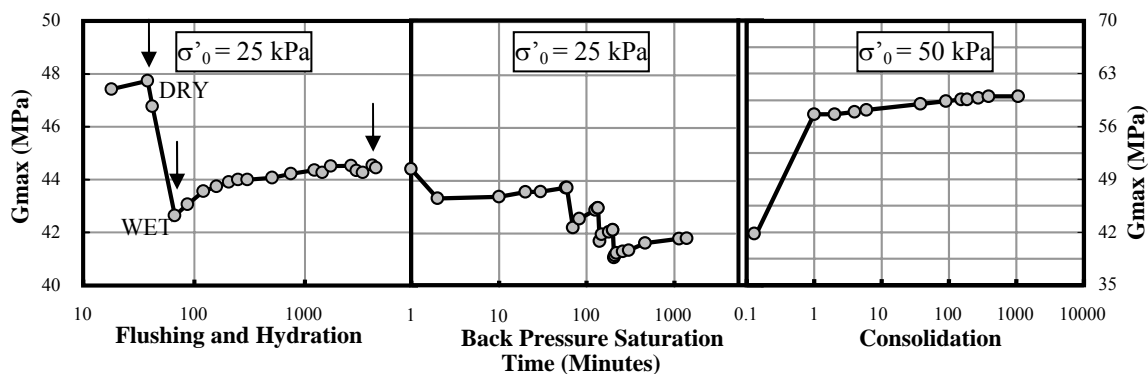


Figure 3: Monitoring of G_{max} throughout the different stages of a resonant column test on a 3% bentonite specimen

not altered during this process resulting in a basically constant stiffness. Over the rest period G_{max} increases slightly.

In contrast to the clean sand, the shear modulus values measured on the 3% bentonite specimen presented in Figure 3 show a sharp drop when the specimen is flushed with water. Over the rest period during which the bentonite hydrates and swells G_{max} shows a continuous increase in stiffness.

Differences in the stiffness measurements between the clean sand specimen and the specimens with bentonite during the flushing and rest period stages of the resonant column tests are highlighted in Figure 4. This figure summarizes the values of G_{max} measured immediately prior to flushing, just after flushing with water and at the end of the 72 hour rest period on the specimens examined in

Figures 2 and 3 (see values in correspondence to three arrows), as well as similar data from a specimen with 5% bentonite. The figure clearly underlines the trends described above for the 0% and 3% specimens and shows that the behaviour of the 5% bentonite specimen is similar to that described for 3% bentonite.

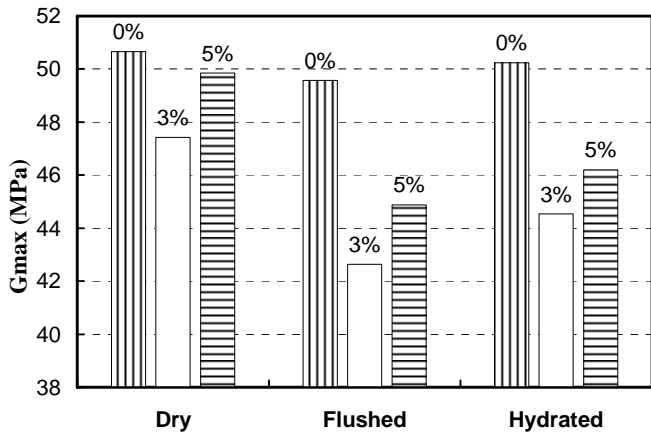


Figure 4: Gmax of 0%, 3% and 5% bentonite specimens at different stages of testing

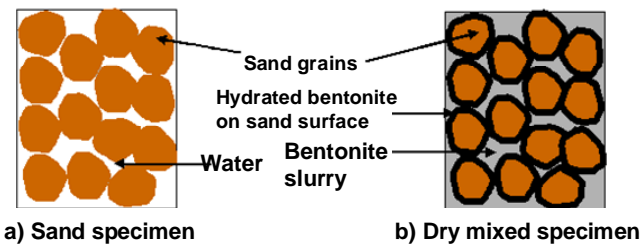


Figure 5: Schematic of fabric of sand and sand-bentonite specimens

The results presented in Figures 2-4 can be interpreted based on the fabric formed in the specimens as a result of the preparation method used. Figure 5 shows a schematic representation of the fabric of a clean sand specimen versus that of a specimen with bentonite. Figure 5b suggests that when the specimens are prepared using the dry mixing method described above, due to the high specific area of the fines, the sand grains are coated with dry bentonite during the mixing process, while the rest of the bentonite occupies the space between the sand grains. Once the bentonite gains access to water, it hydrates and swells. In the pore space this leads to the formation of a pore fluid, which consists of a concentrated bentonite “slurry”. However, the bentonite trapped at the sand particle contacts is prevented from swelling by the contact stresses. When the specimens are dry, the effect of the presence of the dry powder bentonite on the stiffness of the specimen is not significant. It is hypothesized that once hydrated, the bentonite forms a thin layer of a weak soft material that alters the particle to

particle sand contacts and reduces the initial stiffness of the specimens. Hence, it is suggested that despite the small percentage of bentonite present, the fines interfere with the grain to grain contacts giving rise to a fabric that is not completely non-floating.

As shown in Figures 2 and 3, during the back pressure saturation stage, the clean sand and 3% bentonite specimens show very similar behavior: after the first level of back pressure (75 kPa) is applied the stiffness decreases and then starts building up over time. The same behavior is observed for each subsequent back pressure saturation step. This reduction in stiffness (which never exceeds 4% of the initial value of Gmax) can be attributed to the temporary change in effective stresses during the application of the backpressure.

In the tests shown in Figures 2 and 3, consolidation from 25 kPa to 50 kPa occurred in one stage. Figures 2 and 3 show a significant increase in Gmax in the first couple of minutes for both specimens (note the different scale used for Gmax for this stage of the test) due to the increase in confining stress. The stiffness continues to increase over time after that, albeit at a slower rate, as a result of secondary consolidation (aging). An analysis of the effects of aging on Gmax secondary is presented later in the paper.

3.2 Dependence of Gmax on stress level and void ratio

The effects of confining stress and void ratio on the small strain stiffness of soils have been widely studied primarily using the resonant column apparatus (e.g. Hardin and Richart, 1963) and bender elements in a triaxial setup (e.g. Viggiani and Atkinson, 1995). Both techniques involve measuring the shear wave velocity (V_s) and determining the shear modulus from the following equation:

$$G_{max} = \rho V_s^2 \quad \text{eq. 1}$$

where ρ is the total mass density of the soil.

Regardless of the method used to determine the initial shear modulus, the effects of over-consolidation, confining stress, void ratio and soil structure have been well documented. In general the dependence of Gmax on these parameters is expressed using equations such as the one below, with different researchers suggesting different values and formulas for the various parameters.

$$G_{max} = C_g \text{OCR}^k F(e) P_a^{1-n} \sigma_0^n \quad \text{eq. 2}$$

where C_g is a soil structure parameter, OCR is the over consolidation ratio, $F(e)$ is a void ratio function, σ_0 is the effective confining stress, P_a is

atmospheric pressure, and k and n are regression constants.

All tests performed in this study were conducted on normally consolidated ($OCR = 1$) specimens. Given the narrow void ratio range over which the specimens were tested ($e_{bulk} = 0.579$ to 0.692), the results could not be used to calibrate a soil-specific void ratio function. Instead the function shown in eq. 3, and recommended by Hardin (1978) for void ratios ranging between 0.4 and 1.2, was used.

$$F(e) = \frac{1}{0.3 + 0.7e^2} \quad \text{eq. 3}$$

where e is the void ratio of the tested specimen.

Figures 6 and 7 present the values of G_{max} for 0, 3 and 5% bentonite specimens normalized by the void ratio function shown above versus the effective confining stress (both on logarithmic scales). In one case $F(e)$ is calculated from the bulk void ratio, in the second case from the skeleton void ratio. The values C_g and n determined from linear regressions through each of the three data sets are summarized in Table 1. The table presents two sets of data for the 3% and 5% bentonite, and only one set of results for clean sand, as for this material there is no difference between skeleton and bulk void ratio. Note that the values of C_g and n obtained for the clean sand are consistent with results reported in the literature of 625 and 0.5 respectively (Hardin 1978).

A comparison between Figures 6 and 7 indicates that when the skeleton void ratio is used to normalize the G_{max} data the curves for the three soils come closer together, i.e. the skeleton void ratio appears a more appropriate parameter by which to normalize the data. This result is consistent with the fabric of the sand-bentonite specimens, in which the majority of the fines present occupy the voids between the sand grains, and hence does not contribute to the shear stiffness. Similar results have been reported by other researchers for granular mixes with low percentage of fines.

However, as discussed above, due to the specimen preparation procedure employed in this study, the fabric formed in the sand-bentonite specimens is not truly non-floating. As a result of the thin layer of more compressible clay trapped between the sand grains (Figure 5), the values of C_g for the 3% and 5% bentonite specimens (Table 1) are lower than those of the clean sand, reflecting a “softer” structure.

Table 1: Summary of C_g and n parameters

| % Bentonite | Skeletal | | | Bulk | | |
|-------------|----------|-------|-------|-------|-------|-------|
| | C_g | n | R^2 | C_g | n | R^2 |
| 0 | 628 | 0.519 | 0.975 | | | |
| 3 | 548 | 0.557 | 0.992 | 509 | 0.557 | 0.992 |
| 5 | 566 | 0.548 | 0.985 | 501 | 0.548 | 0.985 |

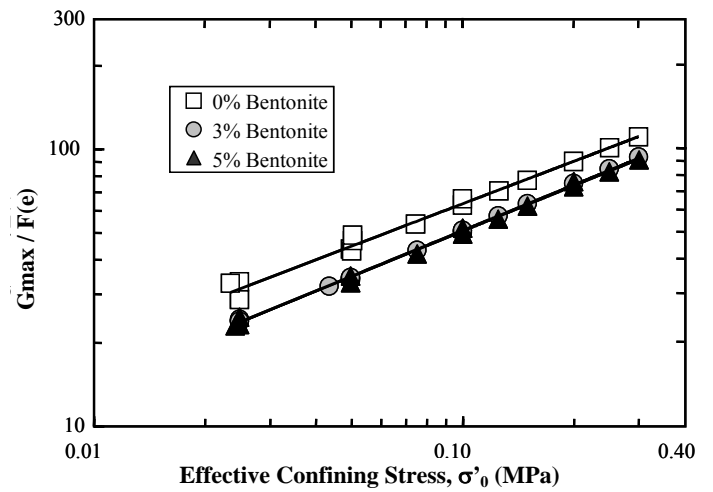


Figure 6: G_{max} normalized by bulk void ratio versus effective confining stress

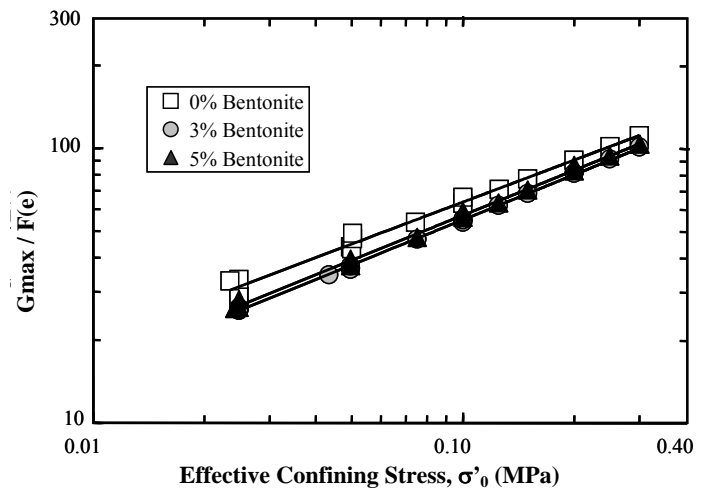


Figure 7: G_{max} normalized by skeleton void ratio versus effective confining stress

Table 1 also indicates that the n values for the 3% and 5% bentonite specimens are higher than that for the clean sand (see also regression lines in Figures 6 and 7). This implies that at higher confining stresses, the shear stiffness of the 3% and 5% bentonite specimens would approach the values of the clean sand. Again, this appears consistent with the fabric hypothesized in Figure 5, as an increase in confining stress would ultimately promote exclusion of the bentonite from the particle contact areas, and direct sand to sand contact.

3.3 Effect of aging on G_{max}

For both clean sand and sand-bentonite specimens, measurements of G_{max} were conducted over time, after the application of the consolidation stresses, to assess the impact of the presence of fines on the increase in stiffness associated with aging (secondary consolidation). A compilation of results from tests performed on specimens consolidated to effective confining stresses in the 50-300 kPa range for times extending to approximately 7 days, is presented in Figure 8. In this figure each of the G_{max} values is normalized by the value of the shear modulus measured on the same specimen 10 minutes after the application of the consolidation stress. Note that for all specimens this time is beyond the end of primary consolidation (which occurs at 0.1 minutes for the clean sand, and approximately 0.3 minutes in the case of the 3% and 5% bentonite specimens). Hence the increase in stiffness measured after 10 minutes reflects only the effects of aging.

Figure 8 presents a regression line through each of the three sets of data. The slope of this line provides the aging coefficient N_G , which quantifies the increase in G_{max} with time and is defined as follows:

$$N_G = \frac{\Delta G_{max}}{G_{max(t=t_{ref})} \log \frac{t}{t_{ref}}} \quad \text{eq. 4}$$

where t_{ref} is a reference time, which in this study is chosen to be 10 minutes; $G_{max}(t=t_{ref})$ is the initial shear stiffness determined at the reference time; t is a generic time, and ΔG_{max} is the increase in shear stiffness at time t with respect to $t=t_{ref}$.

The results presented in Figure 8 show a clear effect of the presence of the bentonite fines on the increase in stiffness associated with aging. While the values of N_G summarized in Figure 8 all fall in the range reported for silicate sands ($N_G = 1-3.5\%$ range, Lo Presti et al., 1996), compared to the clean sand N_G increases by a factor of 2 and of 3 with 3% and 5% bentonite, respectively.

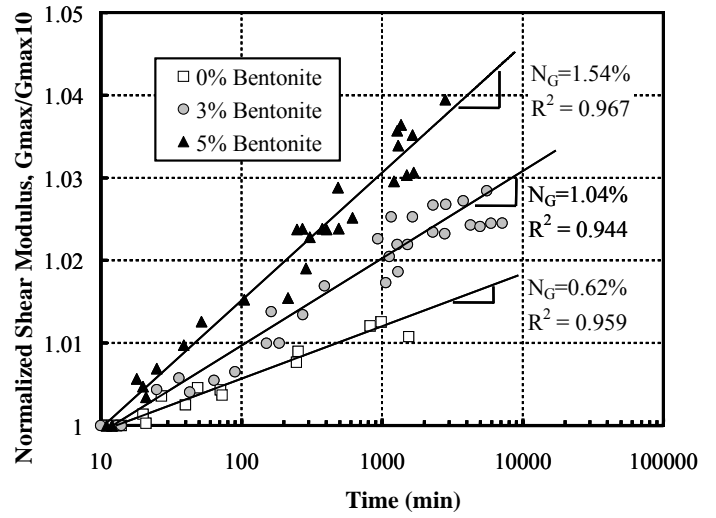


Figure 8: Increase in G_{max} with aging

3.4 Relationship between shear wave velocity and liquefaction resistance

The Drnevich resonant column measures the shear wave velocity while the shear stiffness is calculated using eq. 1. Figure 9 presents the values of the shear wave velocity for the 0, 3 and 5% bentonite specimens versus confining stress. The shear wave velocity values are normalized using the same void ratio function used to normalize the shear modulus values.

The figure shows that for all confining stresses the shear wave velocities of the sand-bentonite specimens are lower than those of the clean sand; as observed for the values of G_{max} , the difference between the clean sand and the sand bentonite specimens decreases with increasing confinement.

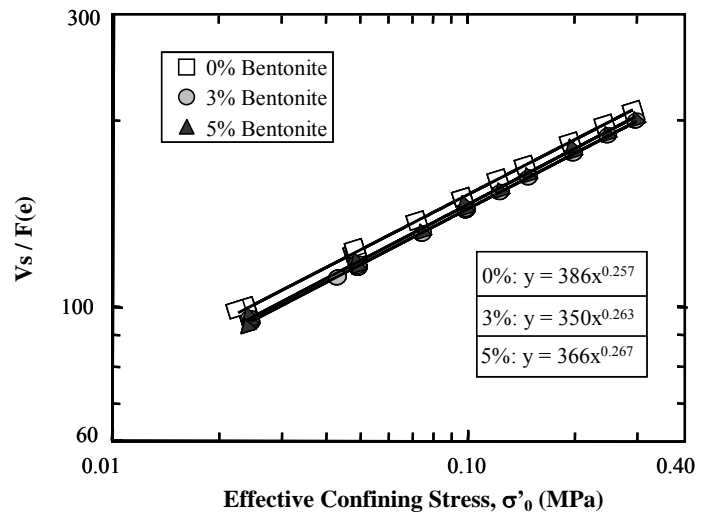


Figure 9: Shear wave velocity normalized by skeleton void ratio versus confining stress

Comparison of the shear wave velocity values for clean sand and sand with bentonite is of interest as recent studies (e.g. Andrus and Stokoe, 2000), have promoted the use of this soil property for evaluating

the liquefaction resistance of soils. Andrus and Stokoe (2000), for example, have proposed correlations between the in situ shear wave velocity (corrected for overburden stresses) and the cyclic resistance of sands with different fines content.

While the shear velocity of the soils with 3% and 5% bentonite is marginally lower than that of the clean sand (Figure 9), it has been shown (El Mohtar et al. 2008) that the presence of 3% and 5% bentonite significantly increases the cyclic resistance of the soil. This result is inconsistent with the use of V_s as an index of liquefaction resistance, and demonstrates the need for a careful characterization of soils when using the shear wave velocity for evaluating liquefaction resistance. The higher liquefaction resistance of the specimens with 3% and 5% bentonite also suggests that in presence of even small percentages of highly plastic fines, procedures such as those proposed by Andrus and Stokoe (2000) may not be applicable.

4 CONCLUSIONS

This paper addresses the effects of plastic fines (bentonite) on the initial (maximum) stiffness (G_{max}) of sand. The study is based on resonant column tests performed on specimens with 0, 3 and 5% bentonite, all with similar skeleton void ratio (corresponding to a skeleton relative density of 35-40%) over a range of consolidation stresses (25-300 kPa) with aging times up to 7 days.

The study shows that a similar relationship of the type $G_{max} = C_g OCR^k F(e) P_a^{1-n} \sigma_0^n$ links G_{max} to skeleton void ratio and effective stress level for all three soils. The presence of fines increases the stress level exponent n and decreases the soil structure factor C_g . The plastic fines also increase the aging coefficient N_g by as much as a factor of 3.

These results can be interpreted based on the microstructure of the sand-bentonite specimens which, despite the small percentage of fines used, is hypothesized to be not completely non-floating. Instead, it is proposed that due to the specimen preparation employed (dry mixing and pluviation and subsequent flushing and saturation of the soil) a thin layer of clay is trapped between the sand grains.

The results illustrate the role played by the specimen preparation method and demonstrate the importance of fully understanding the microstructure and the distribution of the fines as compared to considering only the amount of fines present in a soil.

Finally, the analysis of the shear wave velocities measured on clean sand and sand-bentonite specimens indicates that the use of this parameter as a sole indicator of the liquefaction susceptibility of a soil can be misleading. While this study shows that the sand-bentonite specimens have marginally lower shear wave velocities than the clean sand, a parallel

study conducted on these same soils (El Mohtar et al. 2008) has clearly established that in presence of bentonite the resistance to cyclic loading is greatly increased. Therefore, the use of the shear wave velocity for evaluating liquefaction susceptibility in the field needs to be accompanied by careful soil characterization, and may ultimately find limitations in sand deposits containing even small percentages of highly plastic fines.

ACKNOWLEDGEMENTS

This research was supported by the National Science Foundation, Geomechanics and Geotechnical Systems Program, under grant CMS-0408739. This support is gratefully acknowledged.

REFERENCES

- Andrus, R.D., and Stokoe II, K.H. (2000). "Liquefaction Resistance of Soils from Shear-Wave Velocity", *Journal of Geotechnical and Geoenvironmental Engineering*, v. 126, pp. 1015-1025.
- ASTM D 4015-92 (Reapproved 2000). "Standard Test Methods for Modulus and Damping of Soils by the Resonant Column Method".
- Black, D. K. and Lee, K. L. (1973). "Saturating Laboratory Samples by Back Pressure", *Journal of Soil Mechanics and Foundations Division, ASCE*, Vol. 99, No. SM1, pp. 75-93.
- Carraro, J.A.H., Bandini, P., and Salgado, R. (2003). "Liquefaction Resistance of Clean and Nonplastic Silty Sands Based on Cone Penetration Resistance", *Journal of Geotechnical and Geoenvironmental Engineering*, v. 129, pp. 965-976.
- Drnevich, V.P., Hardin, B.O., and Shippy, D.J. (1978). "Modulus and Damping of Soils by the Resonant-Column Method", *ASTM Special Technical Publication 654, Symposium on Dynamic Geotechnical Testing*, June 28 1977 *ASTM Special Technical Publication*, pp. 91-125.
- El Mohtar, C.S. (2008). "Pore Fluid Engineering: An Autoadaptive Design for Liquefaction Prevention", PhD Dissertation, Purdue University, West Lafayette, IN.
- El Mohtar C.S., Clarke J., Bobet A., Santagata M., Drnevich V. and Johnston C. (2008), "Cyclic Response of a Sand with Thixotropic Pore Fluid", *Geotechnical and Earthquake Engineering and Soil Dynamics IV*, May 18 – 22, 2008, Sacramento, California.
- Finn, W.D.L., Ledbetter, R.H., and Wu, G. (1994). "Liquefaction in Silty Soils: Design and Analysis", *Proceedings of the ASCE National Convention*, Oct 9-13 1994, *Geotechnical Special Publication*, pp. 51-76.
- Georgiannou, V.N., Hight, D.W., and Burland, J.B. (1991). "Behaviour of Clayey Sands under Undrained Cyclic Triaxial Loading", *Geotechnique*, v. 41, pp. 383-393.
- Hardin, B.O. (1978). "Nature of Stress-Strain Behavior for Soils", *Proceedings of the ASCE Geotechnical Engineering*

Division Special Conferences, Earthquake Engineering and Soil Dynamics, Jun 19-21 1978, pp. 3-90.

- Hardin, B.O., and Richart, J. (1963). "Elastic Wave Velocities in Granular Soils", American Society of Civil Engineers Proceedings ASCE Proceedings, Journal of the Soil Mechanics and Foundations Division, v. 89, pp. 33-65.
- Lo Presti, D.C.F., Jamiolkowski, M., Pallara, O. and Cavallaro, A. (1996). "Rate and Creep Effect on the Stiffness of Soils," ASCE Convention, Washington, 10-14 Nov. 1996, Geotechnical Special Publication No.61, pp.166-180.
- Polito, C.P., and Martin II, J.R. (2003), "A Reconciliation of the Effects of Non-Plastic Fines on the Liquefaction Resistance of Sands Reported in the Literature", Earthquake Spectra, v. 19, pp. 635-651.
- Thevanayagam, S., and Martin, G.R. (2002), "Liquefaction in Silty Soils - Screening and Remediation Issues", Soil Dynamics and Earthquake Engineering, v. 22, pp. 1035-1042.
- Thevanayagam, S., Shenthan, T., Mohan, S., and Liang, J. (2002). "Undrained Fragility of Clean Sands, Silty Sands, and Sandy Silts", Journal of Geotechnical and Geoenvironmental Engineering, v. 128, pp. 849-859.
- Vaid, Y.P. (1994). "Liquefaction of Silty Soils", Proceedings of the ASCE National Convention, Oct 9-13 1994, Geotechnical Special Publication, pp. 1-16.
- Viggiani, G., and Atkinson, J.H. (1995). "Stiffness of Fine-Grained Soil at Very Small Strains", Geotechnique, v. 45, pp. 249-265.